Rock Engineering and Technology for Sustainable Underground Construction
Eurock 2012 – the 2012 ISRM International Symposium, 28-30 May 2012, Stockholm, Sweden.

Numerical Investigation of the Influence of Borehole Orientation on Drilling-Induced Core Damage

N. Bahrani
Geomechanics Research Centre, MIRARCO – Mining Innovation, Sudbury, Canada
Bharti School of Engineering, Laurentian University, Sudbury, Canada
B. Valley
Geomechanics Research Centre, MIRARCO – Mining Innovation, Sudbury, Canada
Centre for Excellence in Mining Innovation (CEMI), Sudbury, Canada
S. Maloney
Geomechanics Research Centre, MIRARCO – Mining Innovation, Sudbury, Canada
P.K. Kaiser
Centre for Excellence in Mining Innovation (CEMI), Sudbury, Canada
Bharti School of Engineering, Laurentian University, Sudbury, Canada

Abstract: Damaged and disked core from boreholes are indicators of high stress relative to the intact rock strength at the drilling location. While core disking is mainly used as a means to estimate the in situ stress state, core damage (micro-fractures) and its level need to be identified to allow for the accurate estimation of the in situ intact rock strength and therefore proper design of underground infrastructure such as tunnels and pillars. It is generally recommended that laboratory testing be done on samples from boreholes drilled parallel to the major principal stress. In this study, results are reported from an investigation on the influence of borehole orientation on the drilling-induced core damage and associated strength and modulus reductions. The drilling-induced coring stress paths, for boreholes drilled parallel to σ_1 and σ_3 within a stress state representative for the 420 Level at the Underground Research Laboratory, were first obtained from an elastic three-dimensional finite element model. The coring-induced stress path for the borehole drilled parallel to σ_3 was then applied to a two-dimensional discrete element model previously calibrated to the undamaged Lac du Bonnet granite to create damage in the form of micro-cracks. Once the model was calibrated to both undamaged and damaged LdB granite, it was used to predict the damage level and the unloading-induced micro-crack characteristics of the core from the borehole drilled parallel to σ_1. The results confirm the effect of sample disturbance on rock strength and modulus measured in the laboratory and potentially offer a mean to model this process and quantify drilling-induced core damage.

Theme: Material Models.

Keywords: Drilling-induced core damage, Finite Element Method, Discrete Element Method, stress path, micro-cracks.

1 INTRODUCTION

The intact rock unconfined compressive strength (UCS) and modulus are fundamental parameters required during the course of rock mass characterization. It is recognized that drilling in relatively high stress environments can induce sample disturbance, micro-cracking of the cored samples, which in turn may result in lower values for the intact rock strength and modulus being measured in the laboratory (Martin and Stimpson, 1994). Incorrect estimation of these parameters can lead to costly errors especially during the pre-feasibility stage, when the ability to influence the design of infrastructure such as deep underground openings and pillars is the highest and data are accessible solely from boreholes. Based on field evidence, core disking and core damage are more likely to occur when the boreholes are drilled perpendicular to the maximum principal stress orientation (Martin and Christiansson, 1991).

In recent years, the focus of research was on drilling-induced macro core damage, known as core disking (visible fractures), and less effort was made to better understand the mechanisms involved in initiation and accumulation of micro damage (fractures invisible to the naked eye). The goal of this study was to investigate the influence of borehole orientation on drilling-induced core damage and its impact on the mechanical properties of rock samples being measured in the laboratory. Three-dimensional finite element and two-dimensional discrete element models were used to gain insight into the stress paths experienced by the core during drilling as well as the damage mechanism, and its influence on strength and modulus reduction. The well documented laboratory test results of undamaged and damaged Lac du Bonnet (LdB) granite samples, as well as the in situ stresses representative for the 420 Level at the Underground Research Laboratory (URL), Manitoba, Canada, were used for calibration of numerical models.

2 DRILLING-INDUCED CORE DAMAGE

When a rock core is drilled and retrieved from underground, the state of stress inside the core is changed from the original in situ stresses to the atmospheric condition (Holt et al, 2000). Between these initial and end points, the stress path is dependent on the orientation of the borehole to the principal stress directions as well as the in situ stress magnitudes. As described by Holt et al. (2000) and Zang and Stephenson (2010), in a vertical borehole, the vertical stress is gradually removed from its initial value (Fig. 1a) as the core bit approaches the point P (Fig. 1b). The horizontal stress is then removed when the point P is located inside the core barrel (Fig. 1c). Micro-cracks (Fig. 1b, c and d) can be generated if the deviatoric stress (Fig. 1d) inside the core is high enough ($S_H - S_v >> 0$). The interaction and coalescence of these micro-cracks due to very large deviatoric stresses may result in formation of macro fractures known as core disking.

Evidence of sample disturbance has been documented at the Underground Research Laboratory by Martin and Stimpson (1994) and Eberhardt et al. (1999). They showed that the UCS, Young's modulus, and the P-wave velocity measured on cores decrease and Poisson's ratio increases as samples are obtained at increasing depth and consequently increasing in situ stresses. Interestingly, contrary to the velocity measured on cored samples, the in-situ velocity from sonic logs appeared to be depth independent; sudden drops in velocity were found to be related to the fracture zones.

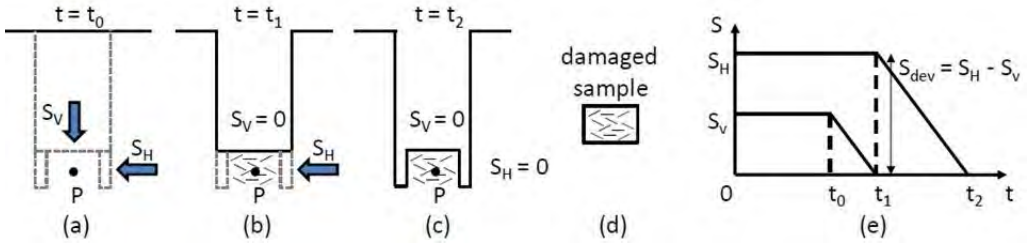

Figure 1. Schematic of core drilling and sample disturbance (modified from Holt et al, 2000, and Zang and Stephansson, 2010): a) far field in situ stresses; b) gradual removal of vertical stress and generation of micro-cracks; c) gradual removal of horizontal stress; d) damaged sample retrieved from the borehole; e) A schematic graph showing stress change inside the core with time and generation of high deviatoric stress.

Similar behavior has also been observed on samples taken from deep mines in South Africa (Watson et al. 2009). Crack counts using Scanning Electron Microscope (SEM) analyses support that samples from greater depths contain larger numbers of micro cracks. Lanaro et al. (2009) reported a strong negative correlation between sample strength and measured in situ stress and explained this observation by sample disturbance. Interestingly, strength reduction in their case was not only a matter of depth but was also related to high stress zones associated with faults.

3 UNDAMAGED VERSUS DAMAGED LAC DU BONNET GRANITE

The Underground Research Laboratory (URL) owned by Atomic Energy of Canada Limited (AECL), constructed between 1983 and 1990, is located within the Lac du Bonnet granite batholiths, about 100 km northeast of Winnipeg, Manitoba, Canada. The extensive in situ stress characterization program using different techniques identified three distinctive stress domains at the URL (Martin, 1990). Stress Domain 1 extends from surface to a depth of 200 m. Stress Domain 2 serves as a transition zone between Domains 1 and 3 and is affected by a main fracture zone. Stress Domain 3, extends to the deepest measurement point at 550 m and is located within the massive grey granite. Typical values of minor and major principal stresses for these three domains are given in Table 1.

Martin and Stimpson (1994) suggested that the change in the laboratory properties of LdB granite is due to the increasing stress-induced damage in the samples with increasing depth (i.e., in-situ stress level). The disturbed samples can be identified from the change in the material response when subjected to uniaxial compression; undamaged samples respond in a linear elastic manner whereas damaged samples initially exhibit a strongly non-linear response due to micro-crack closure (Fig. 2a). These observations were consistent with the results of SEM analyses by Eberhardt et al. (1998) who noted that visible cracks were difficult to find in the thin sections of the samples from the 130 m and 240 m levels, whereas numerous cracks were visible in the 420 Level samples.

Table 1. In situ stress values for the three main domains at the Underground Research Laboratory

Stress Domain	Depth (m)	σ_1 (MPa)	σ_3 (MPa)	σ_2 (MPa)	Reference
1	130	14.2	5.6	8.8	Martin (1990)
2	240	30	12	15	Martin and Christiansson, (1991)
3	420	60	11	45	Martin and Read (1996)

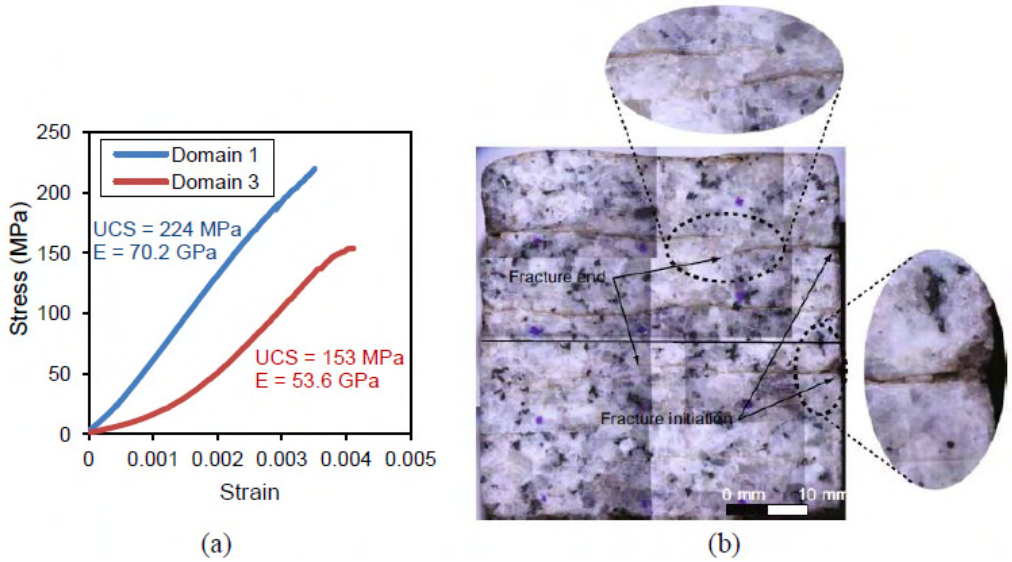

Figure 2. a) Stress strain response of LdB granite samples retrieved from Cold Spring Quarry (Domain 1) and the 420 m level (Domain 3) (Courtesy of Derek Martin), b) initiation and propagation of drilling-induced tensile cracks in a partially disked core (after Lim and Martin, 2010)

According to Martin and Christiansson (1991) stress-induced micro-cracks in LdB granite are identified by their smooth, parallel walls, which would mate perfectly under compressive stress, sharp termination and by a lack of infilling or bridging material. They further explained that the stress-induced micro-cracks in LdB granite are up to 15 μm in width and can be seen with the naked eye. Fig. 2b shows an example of drilling-induced micro-cracks in a partially fractured core of LdB granite.

4 FINITE ELEMENT MODELING OF CORE DRILLING

Three-dimensional elastic analyses were first carried out in order to better understand the stress change within the core during drilling and its variations as a function of borehole orientation relative to the in situ principal stress directions. For this purpose, a 1 m × 1 m × 1 m model (Fig. 3) was built using the finite element code Abaqus (SIMULIA). The simulated core and borehole were 47.6 mm and 75.7 mm in diameter, respectively. The analysis was performed for three borehole orientations: borehole parallel to maximum principal stress (σ_1) or maximum horizontal stress (σ_{Hmax}), borehole parallel to intermediate principal stress (σ_2) or minimum horizontal stress (σ_{Hmin}), and borehole parallel to minimum principal stress (σ_3) or vertical stress (σ_v).

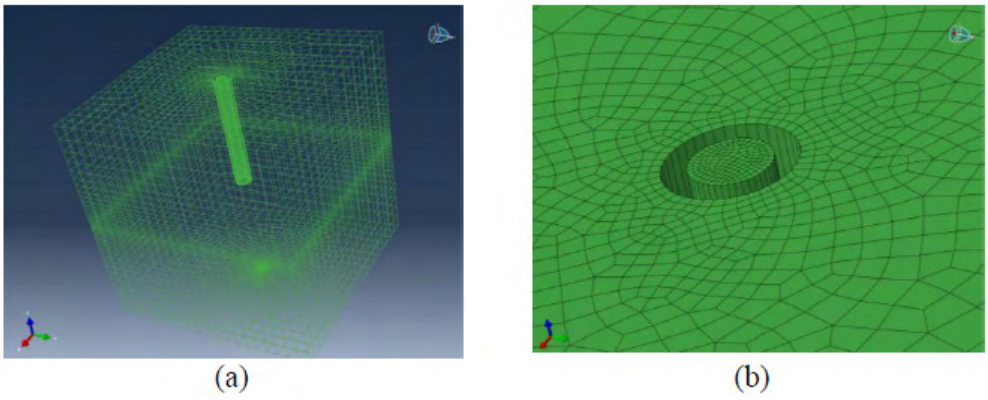

Figure 3. Three-dimensional finite element modeling of core drilling: a) model and borehole geometry, b) close-up view of the collar of the hole.

It should be noted that the damaged samples taken from the URL's 420 Level (Domain 3), were drilled from nearly vertical boreholes (parallel to vertical or minimum principal stress) at depths between 20 to 60 m from the collar, where the influence of excavation disturbance was minimal (Eberhardt, 2010). Therefore, the far field in situ stresses representative for the Domain 3 (σ_1 = 60 MPa, σ_2 = 45 MPa, and σ_3 = 11 MPa) were used as input for numerical analyses. According to Eberhardt et al. (1998), the average UCS of undamaged and damaged samples in Domains 1 and 3 are 213 and 157 MPa, respectively. No information, however, exists on the mechanical properties of the cores obtained from boreholes with other orientations (boreholes parallel to minimum and maximum horizontal stresses) and their possible amounts of damage. Therefore the data available from the cores retrieved from vertical boreholes are used as a baseline to assess and predict the possible amount of damage that may have occurred to those retrieved from horizontal boreholes.

Fig. 4 compares the stress paths experienced by the core during drilling from the three boreholes described above (the median value of eight points across core diameter was used in this figure for comparison). As shown in this figure, the initial stresses are compressive and the cores in all the three cases experience a gradual reduction in minimum (or σ_v) and then maximum (or σ_{Hmax}) principal stresses. In the case of the borehole parallel to minimum principal stress direction (green curve), the maximum principal stress first increases from 60 MPa to about 68 MPa, and then decreases back to 60 MPa when the core is in tension with a maximum tensile stress exceeding the average tensile strength of the undamaged LdB granite. In the borehole parallel to the intermediate principal stress direction (red curve), similar to the vertical borehole, σ_1 increases to slightly less than 68 MPa, but then rapidly decreases to about 60 MPa when σ_3 = 0, and then to 30 MPa with a maximum tensile stress exceeding the average undamaged LdB granite tensile strength. As opposed to these two cases, when the borehole is parallel to the maximum principal stress direction (blue curve), σ_3 is first reduced from 60 MPa to about 50 MPa. The confinement is then gradually removed from the core and reaches zero when the maximum principal stress is nearly 40 MPa. From this point the tensile stress increases and passes the average undamaged LdB granite tensile strength.

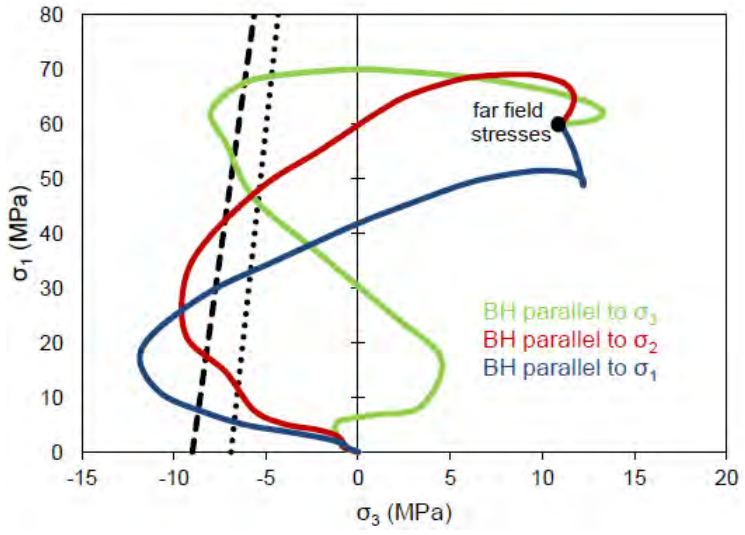

Figure 4. Comparison between stress paths experienced by the core during drilling from boreholes with orientations parallel to in situ principal stress directions. The median stress measured across sample diameter are displayed. Also shown is the failure envelope of undamaged LdB granite passing through its average tensile strength measured from direct tension (dotted line) and Brazilian tests (dashed line).

The main differences between these three cases are the levels of stress anisotropy as well as the magnitudes of tensile stress inside the cores. The maximum deviatoric stress for the borehole parallel σ_3 direction is greater than the crack initiation stress level for LdB granite and greater than those of the cases where the boreholes are drilled parallel to the intermediate (σ_2) and maximum (σ_1) principal stress directions. This suggests that the level of core damage caused by the deviatoric stress is generally greater when the borehole is drilled parallel to the σ_3 direction (σ_V in this case) than the other two cases.

On the other hand, the magnitude of tensile stress inside the core, is highest when the borehole is parallel to σ_1, intermediate when parallel to the σ_2, and lowest when parallel to σ_3. This suggests that the amount of core damage caused by tensile stresses is the highest when the borehole is parallel to σ_1. It is therefore not easy to evaluate the level of core damage based on the stress path obtained from an elastic model. Such an assessment requires a tool that captures not only the three-dimensional stress path, but also the heterogeneous nature of rock and therefore progressive stress-induced fracturing processes and their associate strength and modulus degradation. A possible modeling approach to assist in solving this problem is the Discrete Element Method (DEM).

5 DISCRETE ELEMENT MODELING OF CORE DAMAGE

The Discrete Element Method developed by Cundall (1971) is a numerical method that is capable of simulating particles of any shape for the analysis of rock mechanics problems. It was applied to soils by the implementation of circular particles by Cundall and Strack (1979). DEM has been increasingly used by researchers in the field of geomechanics in recent years. One of the applications of DEM is the simulation of intact rocks and rock masses by considering them as an assemblage of circular or spherical particles, cemented at their contact points (Potyondy and Cundall, 2004). This method, which is called the Bonded Particle Model (BPM), has been implemented in the two- and three-dimensional codes, PFC2D and PFC3D, by Itasca Consulting Group.

The main advantage of the BPM over conventional continuum codes is that predefined complex empirical constitutive relations are replaced with simpler particle contact logic without requiring plasticity rules (Potyondy and Cundall, 2004). Cracking in this method is explicitly simulated as bond breakage. Once a bond breaks, the displacement field as well as the transition to the residual strength are controlled by particle geometry and friction at particle-particle contacts. This explicitly captures a fundamental characteristic of brittle failing rocks known as cohesion weakening/frictional strengthening (Martin and Chandler, 1994; Hajiabdolmajid et al, 2002). The concept of cohesion weakening/frictional strengthening for brittle rocks was captured by Martin and Chandler (1994) who showed that with increasing damage the cohesional strength component is gradually lost and the frictional strength component mobilized.

The clumped particle model suggested by Cho et al, (2007) was chosen to simulate the cracking process occurring in the core during drilling with different borehole orientations. A clump consists of more than one particle but moves as a single rigid object. Therefore, the irregular shape of a rock grain is captured more realistically than the conventional bonded particle model. Cho et al. (2007) used the clumped particle model and found excellent agreement between the failure envelope predicted by PFC and that of the LdB granite. Holt et al. (2003) also found that the elongated particles generated by clumping two particles to generate a rigid irregular object rather than circular or spherical particles improve the simulation results.

Cho et al. (2007) proposed an algorithm to generate a clumped particle model by which a clump can be created by stamping a circled area that corresponds to a desired grain size. In this approach the particles with their centre points located within the circles are added to a clump. This algorithm was adopted to convert the conventional bonded particle model to the clumped particle model in a 3.17 cm × 6.34 cm sample. The average clump size (clump diameter) of 2 mm was chosen to be equal to the average grain size of LdB granite. A total of 6 models with different particle seeds were generated and the average values of the simulation test results were compared with the actual test results. A systematic calibration process was undertaken, which involved: 1. calibration of undamaged LdB granite σ_1, UCS and E, 2. application of an approximate coring-induced stress path to the calibrated model, and 3. calibration of damaged LdB granite UCS and E. The procedure employed for the calibration is shown in the form of a flow chart in Fig. 5. A detailed description of the calibration process has been provided by Bahrani et al. (2011).

The approximate stress path, shown in Fig. 6, is representative of core retrieval from a vertical borehole. It is similar to that utilized by Holt et al. (2000) for the creation of drilling-induced damage to a synthetic sandstone sample in the laboratory. As illustrated by this figure the applied stress path only captures the unloading that occurs under an overall compressive stress field. Therefore the damage resulting from this process is only caused by the deviatoric stress but not by induced tensile stresses in the cored sample.

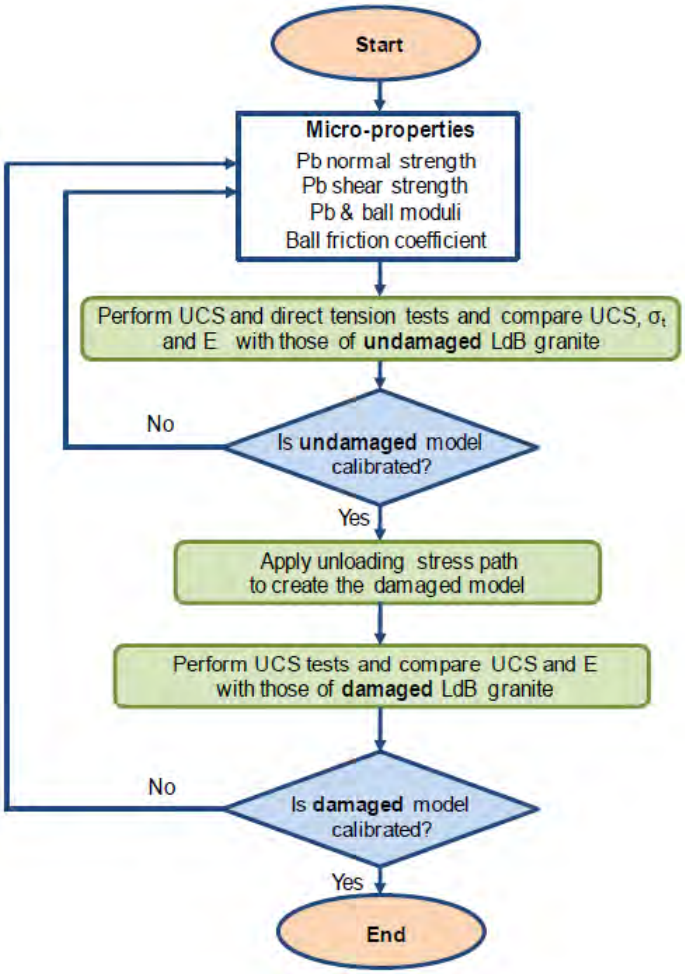

Figure 5. Procedure for calibrating the clumped particle model to the laboratory properties of both undamaged and damaged LdB granite (after Bahrani et al., 2011).

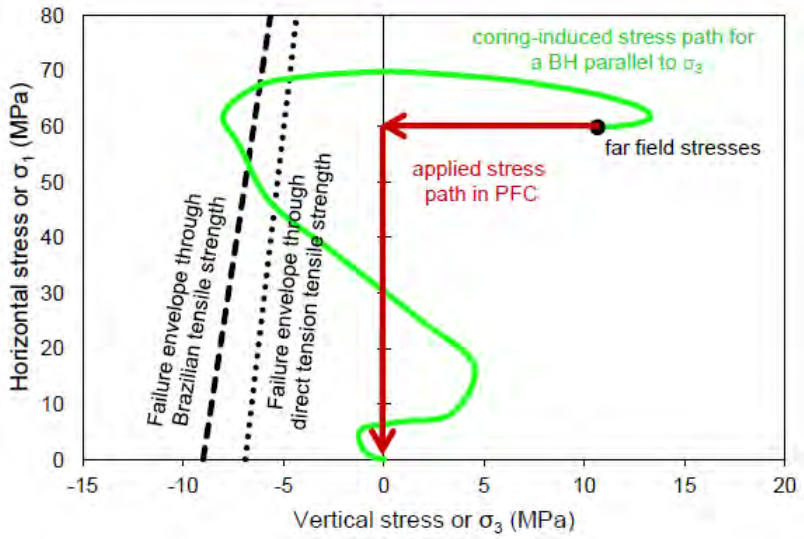

Figure 6. Approximate stress path applied to PFC model to simulate the stress path in the core drilled from a borehole parallel to σ_3.

6 CALIBRATION RESULTS

6.1 Borehole parallel to minimum principal stress

Table 2 lists the micro-properties of the clumped model calibrated to laboratory properties of both undamaged and damaged LdB granite. In this table, R_{min} is the minimum particle radius, R_{max}/R_{min} is the ratio of maximum to minimum particle radius, k_n/k_s and $\bar{k}^n/\bar{k}^s$ are the contact and parallel bond stiffness ratios (normal to shear). E_c and $\bar{E}_c$ are the contact and parallel bond moduli, respectively. $\bar{\lambda}$ is the parallel bond radius multiplier and μ is the particle friction coefficient. $\bar{\sigma}_n$ and $\bar{\sigma}_s$ are the parallel bond normal and shear strengths, respectively.

Table 3 compares the laboratory tests and PFC calibration results for both undamaged and damaged LdB granite. For the PFC results, mean and standard deviation values are obtained by averaging the simulation test results of 6 models with different particle seeds (i.e. different ball arrangements but the same micro-properties as listed in Table 2). As can be seen in Table 3 an excellent agreement exists between the actual test and numerical simulation results for both the mean values and their standard deviations.

Table 2. Micro-properties of LdB granite in the clumped particle model

Micro-parameters	Values	Micro-parameters	Values
R_{min}	0.2 mm	μ	0.3
R_{max}/R_{min}	1.5	$\bar{\lambda}$	1
k_n/k_s and $\bar{k}^n/\bar{k}^s$	2.5	$\bar{\sigma}_n$	12 ± 1.2 MPa
E_c	15 GPa	$\bar{\sigma}_s$	155 MPa
$\bar{E}_c$	18 GPa	Clump radius	1 ± 0.2 mm

Table 3. Comparison between laboratory and PFC simulation test results for undamaged and damaged LdB granite.

Parameters	Laboratory test results	PFC results
Undamaged UCS (MPa)	213 ± 20	211.5 ±12.7
Undamaged E (GPa)	65± 5	65.4 ± 2.85
Undamaged σ_t (MPa)	6.9 ±1	7.2 ± 0.2
Damaged UCS (MPa)	157.1 ± 17.7	157.9 ± 17.7
Damaged E (GPa)	51.9 ± 1.6	48 ± 2.48

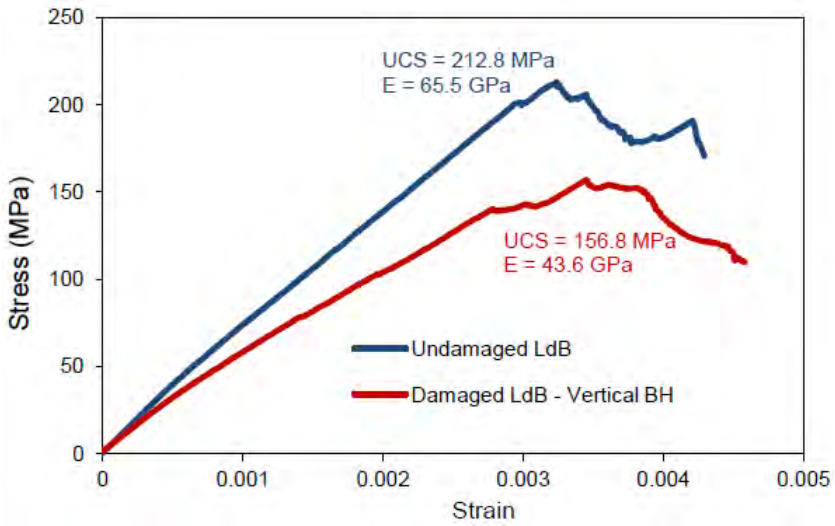

Figure 7. Comparison between PFC predicted stress-strain curves for undamaged and damaged LdB granite samples after applying the approximate stress path of a core drilled from a borehole parallel to σ_3.

The stress-strain curves of the undamaged and damaged clumped particle models are shown in Fig. 7. Although the strength and modulus reductions were properly captured, the damaged model fails to simulate the non-linear portion of the stress-strain curve observed in the damaged LdB sample (compare Fig. 2a and Fig. 7). This is because crack opening during unloading and thus crack closure while reloading is not captured in the model (i.e., the model is cracked but the cracks do not open).

6.2 Borehole parallel to maximum principal stress

Once the models were calibrated to both undamaged and damaged LdB granite samples (with simulated coring-induced stress path in the borehole parallel to σ_3), the approximate stress path of a core retrieved from a borehole parallel to the σ_1 direction was applied to the undamaged model. As shown in Fig. 8, similar to the case of the vertical borehole, the approximate stress path does not simulate the actual unloading that occurs in the tensile stress field.

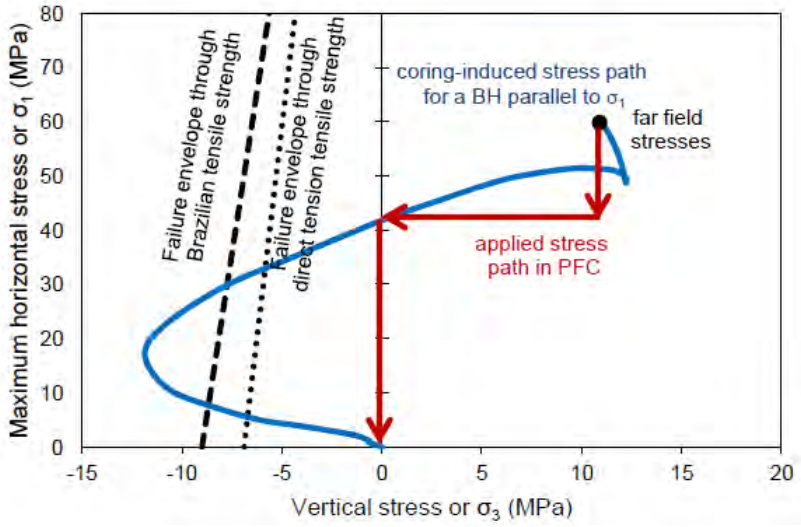

Figure 8. Approximate stress path applied to PFC model to simulate the stress path in the core drilled from a borehole parallel to σ_1.

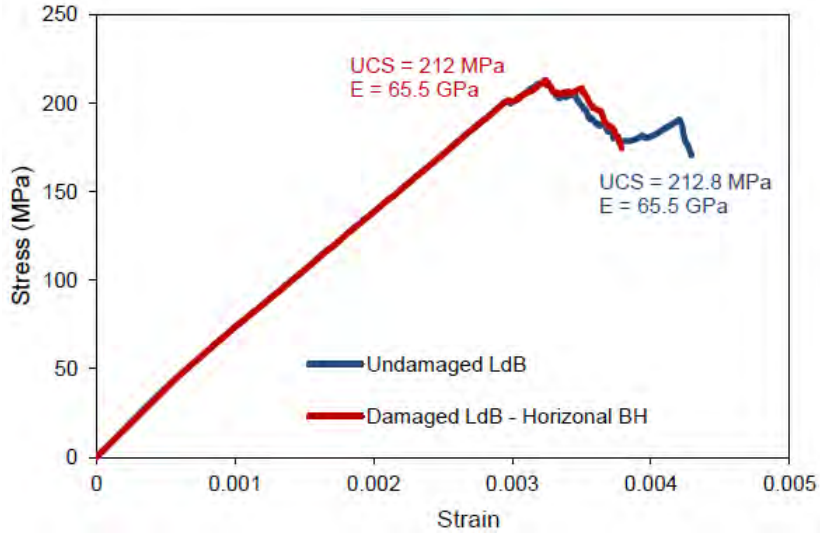

Figure 9. Comparison between PFC predicted stress-strain curves for undamaged and damaged LdB granite samples after applying the approximate stress path of a core drilled from a borehole parallel to σ_1.

Fig. 9 compares the stress-strain curves of the undamaged model and the model with the applied coring-induced stress path of a borehole parallel to σ_1 direction. As can be seen, the stress-strain curves as well as the calculated UCS and E of these two models are essentially the same. Only the post-peak behaviors are slightly different.

7 UNLOADING- AND RELOADING-INDUCED MICRO-CRACKING

Fig. 10a and Fig. 10c compare the micro-cracks generated inside the clumped models during the unloading stages for boreholes parallel to σ_3 and σ_1 directions, respectively. As can be seen the unloading-induced micro-cracks are tension cracks and randomly located in the clumped models in both cases.

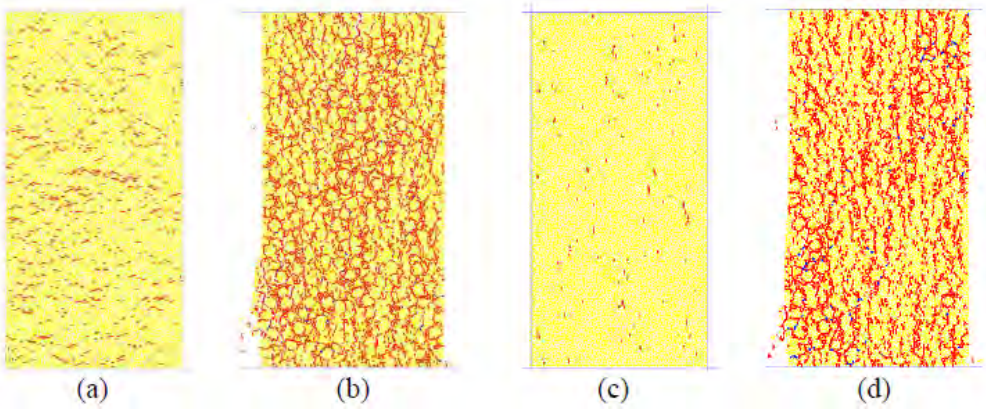

Figure 10. a) Unloading-induced micro-cracks in the case of a borehole parallel to σ_3, b) micro-cracks generated from the beginning of the test up to 70% of the peak in the post-peak region, in the case of borehole parallel to σ_3, c) unloading-induced micro-cracks in the case of a borehole parallel to σ_1, b) micro-cracks generated from the beginning of the test up to 70% of the peak in the post-peak region, in the case of a borehole parallel to σ_1. Red and blue indicate tensile and shear cracks, respectively.

The orientations of these cracks are nearly perpendicular and parallel to the sample axes in the cases of boreholes parallel to the σ_3 and σ_1 directions, respectively. It is clear that the core retrieved from the vertical borehole (i.e., borehole parallel to σ_3) is more damaged and therefore expected to be weaker and softer compared to the core retrieved from the horizontal borehole (i.e., borehole parallel to σ_1).

The locations, orientations and genesis (shear or tensile) of all the cracks formed in the clump models from the beginning unloading stage to the end of axial loading (70% of the peak strength in the post-peak region), in the cases of boreholes parallel to the σ_3 and σ_1 directions are illustrated in Fig. 10b and Fig. 10d, respectively. The cracks in the case of the borehole parallel to σ_1 are oriented approximately parallel to the sample axis, whereas cracks with orientations parallel and perpendicular to the sample axis can be seen in the case of the borehole parallel to σ_3. The difference in the orientations of micro-cracks in these two cases suggests that cracks perpendicular to the sample axis generated during the unloading stage in the case of the borehole parallel to σ_3 (i.e., vertical borehole) and their interaction with cracks parallel to sample axis, formed during axial reloading, resulted in the failure of the sample at a lower stress compared to the case of the unloading stress path representative for the borehole parallel to σ_1 direction. A few inclined shear cracks can also be identified in both cases. These shear cracks initiated just before the peak stress and mainly accumulated in the post-peak region in both cases. The interaction between tensile and shear cracks drive the clump models to failure.

8 CONCLUSION

The investigation on the influence of borehole orientation on drilling-induced core damage using 3D finite element code Abaqus and 2D discrete element code PFC led to the following conclusions:

- Core retrieved from borehole parallel to σ_3 experience higher stress anisotropy than those retrieved from boreholes parallel to σ_1 and σ_2.
- Core retrieved from borehole parallel to σ_1 experience higher tensile stress than those from boreholes parallel to σ_3 and σ_2.
- Micro-cracks in the core retrieved from borehole parallel to σ_3 are oriented nearly perpendicular to the sample axis.

- Micro-cracks in the core retrieved from borehole parallel to σ1 are oriented sub-parallel to the sample axis.
- Sample retrieved from borehole parallel to σ3 is more damaged and therefore weaker and softer than that retrieved from borehole parallel to σ1.
- The use of a modeling technique that simulates damage initiation and accumulation, here a clumped particle model in PFC2D, allows to capture most of these observed effects.

The numerical simulation results presented in this paper suggest that rock strength measured in the lab from samples retrieved from high stress fields should be treated with caution. Other methods of rock strength evaluation such as borehole geophysics and back analysis of borehole breakouts along with laboratory testing may deliver better estimates of the in situ intact rock strength. The analysis results reported here confirm the effect of sample disturbance on rock strength and modulus measured in the laboratory and potentially offers a mean to model this process and quantify the drilling-induced core damage.

9 ACKNOWLEDGEMENTS

This research project is supported by Rio Tinto, Natural Sciences and Engineering Research Council of Canada (NSERC) and Itasca Consulting Group. The authors would like to thank Derek Martin and Erik Eberhardt for discussions at different stages of manuscript preparation. The technical advice received from Matthew Pierce, David Potyondy and Sacha Emam from Itasca Consulting Group is thankfully acknowledged.

10 REFERENCES

Bahrani N., Valley B., Kaiser P.K. 2011. Discrete element modeling of drilling induced core damage and its influence on laboratory properties of Lac du Bonnet granite, In: *Proc. 45th US Rock Mech. Symp.*, San Francisco, Paper 350, 9p.

Cho N., Martin C.D. and Sego D.C. 2007. A clumped particle model for rock. *Int. J. Rock Mech. Min. Sci.*, 44: 997-1007.

Cundall P.A. 1971. A computer model for simulating progressive, large scale movements in blocky rock systems, In: *Proc. Symp. Int. Soc. Rock. Mech.*, Nancy 2, No. 8.

Cundall P.A., Strack O.D.L. 1979. A discrete numerical model for granular assemblies, *Geotechnique*, 29(1): 47-65.

Eberhardt E., 2010. Personal communication.

Eberhardt E., Stead D. & Stimpson B. 1999. Effects of sample disturbance on the stress-induced microfracturing characteristics of brittle rock. *Canadian Geotechnical Journal*, **36**: 239-250.

Hajiabdolmajid, V., Kaiser, P. K., and Martin, C. D., 2002. Modelling brittle failure of rock. *Int. J. Rock Mech. Min. Sci.*, 39 (6): 731-741.

Holt R.M., Brignoli M. and Kenter C.J. 2000. Core quality: quantification of coring-induced rock alteration. *Int. J. Rock Mech. Min. Sci.,* 37: 889-907.

Holt RM, Doornhof D, Kenter CJ. 2003. Use of discrete particle modeling to understand stress-release effects on mechanical and petrophysical behavior of granular rocks. In: Konietsky H (ed), *Numerical modeling in mictomechanics via particle methods*. Swers & Zeitlinger, Lisse, pp 269-276.

Lanaro F., Sato T. & Nakama S. 2009. Depth variability of compressive strength test results of Toki granite from Shobasama and Mizunami Construction Sites, Japan. *Rock Mechanics and Rock Engineering*, **42**: 611-629.

Lim S.S. and Martin C.D. 2010. Core disking and its relationship with stress magnitude for Lac du Bonnet granite. *Int. J. Rock. Mech. Min. Sci. & Geomech. Abstract*. 47 (2): 254-264.

Martin C.D. 1990. Characterizing in situ stress domains at the AECL Underground Research Laboratory. *Can. Geotech. J.*, 27: 631-646.

Martin C.D. and Read R.S. 1996. AECL's mine by experiment: a test tunnel in brittle rock. In: *Proc. 2nd North American Rock Mech. Symp.*, Montreal, eds. Aubertin et al., Vol. 1, p. 13-24.

Martin C.D. and Stimpson B. 1994. The effect of sample disturbance on laboratory properties of Lac du Bonnet granite. *Can. Geotech. J.*, 31: 692-702.

Martin, C.D. and Christiansson, R. 1991. Overcoring in highly stressed granite - the influence of microcracking. *Int. J. Rock. Mech. Min. Sci. & Geomech. Abstract*. 28 (1): 53-70.

Potyondy D.O. and Cundall P.A. 2004. A bonded particle model for rock. *Int. J. Rock Mech. Min. Sci.*, 41: 1329-1364.

Watson B.P., Kuijpers J.S., Henry G., Palmer C.E. & Ryder J.A. 2009. Nonlinear rock behaviour and its implications for deeper level platinum mining. *The Journal of South African Institute of Mining and Metallurgy*, **108**: 5-13.

Zang A. and Stephansson O. 2010. *Stress Field of Earth's Crust*, Springer, 342 p.